Hindawi
Geofluids
Volume 2022, Article ID 8562226, 12 pages
https://doi.org/10.1155/2022/8562226

Research Article

Experimental Investigation on Influence of Acidic Dry-Wet Cycles on Karst Limestone Deterioration and Damage

Yan Zhang[1], **Zicheng Wang**[1], **Guoshao Su**[2], **Zhekang Wu**[1] and **Fengtao Liu**[1]

[1]*Guangxi Key Laboratory of Geomechanics and Geotechnical Engineering, College of Civil Engineering and Architecture, Guilin University of Technology, Guilin 541004, China*
[2]*Guangxi Key Laboratory of Disaster Prevention and Engineering Safety, College of Civil Engineering and Architecture, Guangxi University, Nanning 530004, China*

Correspondence should be addressed to Fengtao Liu; celiuft@glut.edu.cn

Received 17 February 2022; Accepted 2 June 2022; Published 1 July 2022

Academic Editor: Meng Jingjing

This study is aimed at the problem of limestone deterioration and damage caused by the combination of acid rain and the dry-wet cycle in Guilin. Samples of limestone were taken to study the influence of acidic dry-wet cycles on limestone deterioration and damage. This was accomplished by performing nuclear magnetic resonance (NMR) measurements and inductively coupled plasma atomic emission spectrometer measurements on the limestone samples. The study found that with an increase in the number of cycles, the T_2 curve of the rock continuously shifts to the right, but the range of movement still decreases with pH increasing values. The T_2 spectrum area, rock porosity, porosity deterioration, mass loss rate, and water absorption rate all increase with an increase in the number of cycles, but the growth rate continues to decrease, and the increase is negatively correlated with pH. After the dry-wet cycles, the mass concentration of each element in the beaker is Ca, Mg, and Fe in order from high to low, and the mass concentration of each main element in the reaction solution increases with the increase in the number of acidic dry-wet cycles.

1. Introduction

Karst landscapes are gradually suffering from human activity and climate change, and the acceleration of karst landscape degradation in Guilin caused by acid rain is noticeable [1, 2]. Owing to the adverse effect of acid rain, some active minerals in rocks will be dissolved, and mineral dissolution often produces microstructural variations that change the macroscale properties, such as permeability, porosity, pore size distribution, strength, hardness, fracture characteristics, and creep [3–10]. In addition, more than 70% of the rainfall occurred from April to August according to the recorded data from 1951 to 2019 in Guilin [1]. Therefore, a rock mass is usually in a state of wetting and drying cycles, and the damage and deterioration of the rock mass caused by this cyclic change is often more serious than that of sustained immersion [11–20].

In recent years, numerous studies on the damage and mechanical properties of rock masses under dry-wet cycles have been carried out. Obert et al. [21] and Hawkins and McConnell [22] studied the influence of water content on the mechanical properties of sandstones. Through uniaxial compressive strength tests, the results show that the compressive strength of sandstone decreases with increasing of water content. Studies on the mechanical parameters and micromorphological characteristics of sandstone under dry-wet cycles have been probed [23–25], and the results demonstrate that the fracture toughness, elastic modulus and other parameters of sandstone will decrease to a certain extent with the increase in the number of cycles. At the same time, it will be accompanied by large growth in crack speed. Experimental investigation on the effect of dry-wet cycles on mudstones also shows that the porosity of the rock continued to increase and the shear strength continued to decrease with an increasing number of cycles [26, 27].

Influenced by acid rain and cyclic wetting and drying, the deterioration of limestone rock mass will be severe, which makes it more prone to instability and karst collapse

Table 1: Limestone mineral content.

Ingredient	Calcite	Quartz	Dolomite	Mica
Mineral composition%	96	2	1	1

Figure 1: Limestone samples.

in Guilin [28–33].To effectively prevent the deterioration of and damage to limestone in Guilin, which may cause losses to people's lives, property and economy, it is very important to comprehensively investigate the mechanisms of degradation and damage of limestone in the case of the acidic dry-wet cycle. However, to date there are still few studies on the influence of the combination of acid rain and dry-wet cycles on the deterioration and damage of limestone in the literature. Therefore, the experimental investigation of the mechanical behaviors of limestone with acidic dry-wet cycles is carried out by using a nuclear magnetic resonance(NMR) instrument, inductively coupled plasma atomic emission spectrometer, and other equipment. Detailed observations describe the physical and chemical phenomena that occur during the acidic dry-wet cycle. Through data analysis and image comparison, the corrosion and degradation mechanism of limestone during acidic dry-wet cycles is analyzed and compared.

2. Test Setup and Procedure

2.1. Test Materials. The limestone samples used in this test are taken from Qixing Mountain in Guilin City. The rock masses are grayish white or light gray and moderately weathered, and the rock texture is hard and brittle. The samples here are called "oolitic" limestone. X-ray diffractometer was employed to carry out the qualitative and quantitative analysis of limestone minerals. The limestone samples are ground into a fine powder and placed in the instrument. Then, the main constituents of the rock are tested. The results are shown in Table 1.

By referring to the recommended specifications of the International Society of Rock Mechanics (ISRM) [34], the rock samples are, therefore, drilled, cut, and ground into cylinders with a diameter $D = 50$ mm and a height $H = 100$ mm, with an allowable deviation of less than 0.3 mm in both diameter and height. Then, the samples are polished so that the deviation of unevenness at both ends is less than 0.05 mm, and the end face is perpendicular to the axis.

The selected limestone is large in size and integral in structure. Prior to processing the sample, it is subjected to ultrasonic nondestructive testing to screen out those samples with weathering fissures. In an effort to avoid the potential dispersion of the results incurred by the inhomogeneity of limestone samples, the number of samples undergoing the same number of dry-wet cycles at the same pH is three, and together with those in the control group in the natural state, a total of 30 rock samples are selected in this experiment (Figure 1).

2.2. Test Procedure. Taking group Q as an example, limestone samples are dried continuously at 105°C for 24 hours in a constant temperature oven and then soaked naturally in pH = 3 acidic aqueous solution (3 : 1 sulfuric acid + nitric acid) for 48 hours after cooling. The established dry-wet cycles in the process are derived by referring to the relevant test results [12–14]. Limestone samples numbered in the Q group are tested for $n = 1$, 5, and 10 dry-wet cycles. To compare and study the influence of the acid dry-wet cycle on limestone, the same test method as the Q group is used to test groups Z and D. Only an acid solution with pH = 5 (the configuration method is the same as above) and distilled water with pH = 7 are used for the dry-wet cycle, and the limestone samples labeled M are the natural control group. Given that the pH value of rainwater in the Guilin area ranges from 3.44 to 7.03, it is therefore reasonable to select solutions within this range and of these three pH values for the test. After 1, 5, and 10 cycles of acid dry-wet cycles, two samples from groups Q, D, and Z were taken for NMR testing, and the stock solution of limestone samples was diluted to detect the concentration of metal elements in the reaction solution. The instrument used in the NMR test is shown in Figure 2(a). With the help of an inductively coupled plasma atomic emission spectrometer, the concentrations of elements in the reaction solution after the dry-wet cycle were detected. The equipment used is shown in Figure 2(b). The experimental design is shown in Figure 3.

The specific numbering method of limestone samples used in the test is shown in Table 2.

3. Analysis of Experimental Results

3.1. Comparative Analysis of NMR Measurement Results

3.1.1. Analysis of the T_2 Spectrum Distribution. Recent years have witnessed the wide application of NMR techniques in the fields of rock physical properties and porosity. The principle of the technique is that the relaxation time of atomic nuclei under the action of an applied magnetic field is measured and then is fit to a mathematical model to generate an NMR spectrum that can be studied further. In the process of rock NMR measurement, the pores of the rock are filled with fluid. The lateral relaxation time T_2 of the fluid measured by the NMR technique can reflect the sizes of pores and cracks inside the rock. Referring to the positive proportional relationship between the T_2 spectrum area and pore fluid volume, a valid porosity less than or equal to that of the rock sample can therefore be obtained. According to the basic

(a) (b)

Figure 2: Test equipment. (a) Large aperture NMR imaging analyzer. (b) Inductively coupled plasma atomic emission spectrometer.

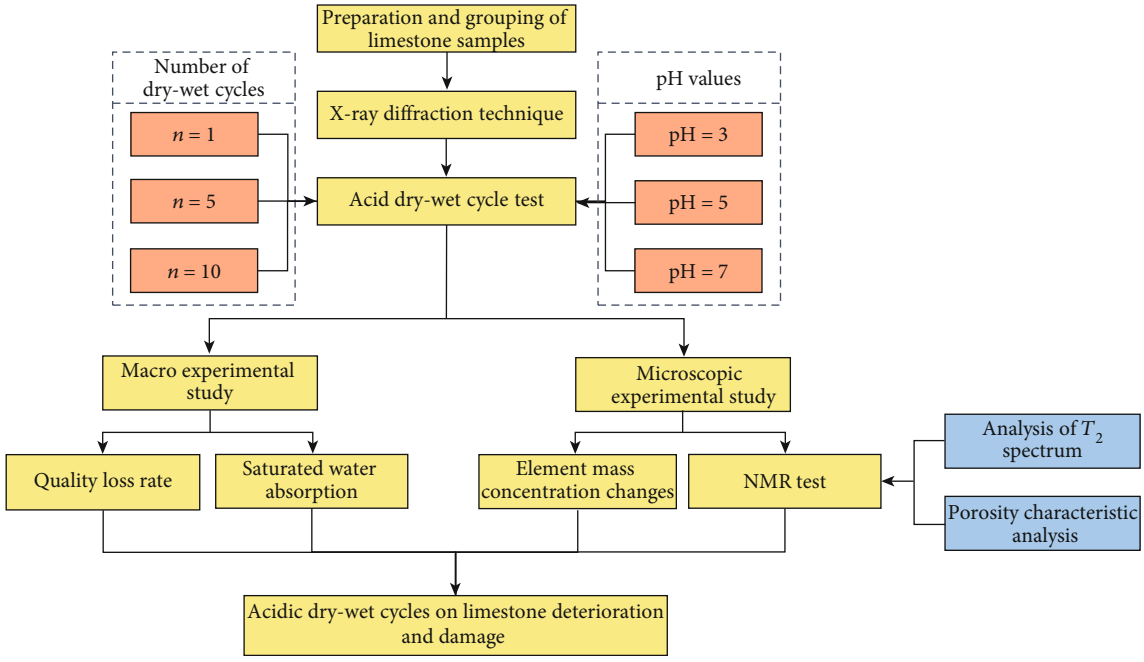

Figure 3: Flow chart of the experimental design.

Table 2: Limestone sample numbering method.

Limestone sample size(mm × mm)	Treatment method	Sample identifier	Number of samples
φ100 × 50	Natural state	M-0	3
	pH = 3	Q-1	9
		Q-5	
		Q-10	
	pH = 5	Z-1	9
		Z-5	
		Z-10	
	pH = 7	D-1	9
		D-5	
		D-10	

principles of NMR, the characteristics of the T_2 spectrum curve reflect the size and distribution of the pores of the specimen, where the position of the peak is related to the size of the pore, and the area of the peak is related to the number of pores. Two specimens in each group are selected for NMR measurement, and the T_2 distribution under different pH environments and different numbers of dry-wet cycles is compared, as shown in Figure 4.

The T_2 spectrum curve of each limestone sample shown in Figure 4 has moved to the right by varying degrees after the dry-wet cycle. According to Figure 4, the move-to-the-right phenomenon is the most obvious at pH = 3, followed by pH = 5, and pH = 7 is the least obvious. This shows that with increasingly acidic conditions, the overall pore size of the rock tends to increase. In addition, at the condition of the same pH value, with the increase in the number of dry-wet cycles, the T_2 spectrum curve continues to move to the right, but the range of motion gradually decreases, indicating that each dry-wet cycle will cause expansion of

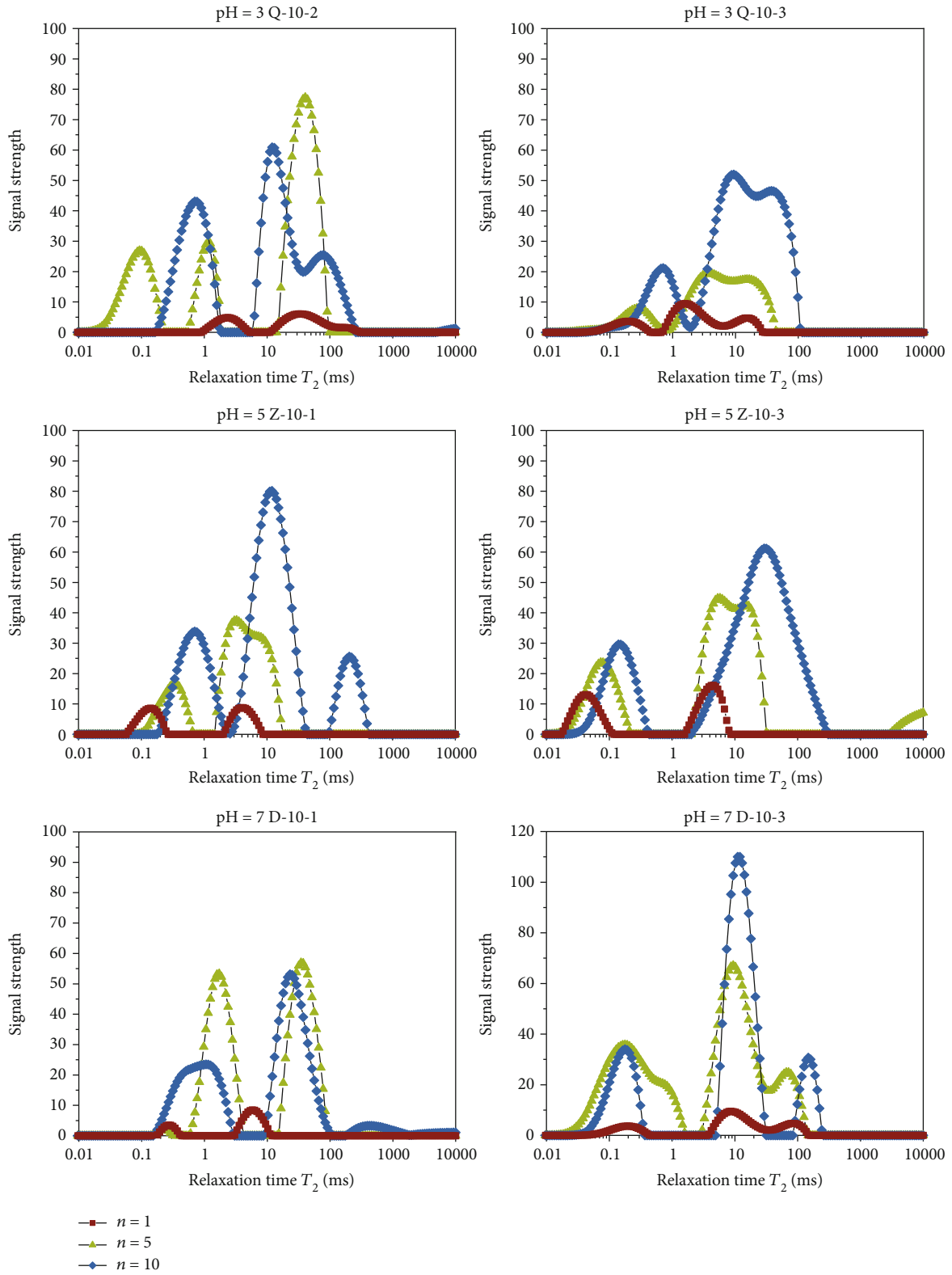

Figure 4: Variation in the T_2 spectrum distribution of limestone under different dry-wet cycles and different pH values.

old cracks and formation of new pores. Moreover, the rate of new pore generation continuously decreases.

Most NMR T_2 curves in Figure 4 show 2~3 peaks. When there are 3 peaks, the pores corresponding to these three peaks are micropores, small pores, and large pores in order from left to right. The pores in the rock are distributed with few small pores and large pores, but small pores account for the main part. After the first dry-wet cycle, the

Table 3: T_2 spectrum area under different operating environments and different numbers of dry-wet cycles.

Active environment	Number	Total peak area	Percentage of peak area/%		
			First peak	Second peak	Third peak
pH = 3	Q-10-2-1	195.285	32.975	62.325	4.7
	Q-10-2-5	1882.802	23.196	14.741	62.063
	Q-10-2-10	2055.573	36.021	43.001	20.668
	Q-10-3-1	275.908	21.029	57.675	21.296
	Q-10-3-5	1679.041	20.236	42.529	37.235
	Q-10-3-10	2180.602	16.724	48.767	34.508
pH = 5	Z-10-1-1	202.799	49.511	50.489	_
	Z-10-1-5	1932.526	58.616	41.384	_
	Z-10-1-10	2393.511	25.149	62.683	12.168
	Z-10-3-1	275.728	47.631	52.369	_
	Z-10-3-5	1624.719	24.801	42.81	28.171
	Z-10-3-10	1963.584	30.042	69.958	_
pH = 7	D-10-1-1	115.524	21.103	77.816	1.08
	D-10-1-5	1556.554	0.014	0.856	47.785
	D-10-1-10	1492.498	38.256	56.66	3.99
	D-10-3-1	145.877	27.377	48.256	24.367
	D-10-3-5	2648.225	41.109	46.792	12.099
	D-10-3-10	2277.309	21.989	66.631	11.379

peak value of each spectrum signal does not exceed 10. With the increase in the number of dry-wet cycles, the signal peaks increase to varying degrees, and the increase in the main peak is particularly pronounced. This shows that during the dry-wet cycle, pores of different sizes within the rock are developed, but the development and expansion of small-sized pores are faster than those of the micropores and large-sized pores.

After the fifth dry-wet cycle, the peak signal strength increased the most. As the number of dry-wet cycles increases, the upward trend gradually decreases. The reasons for these results are as follows: in the early stage of the dry-wet cycle, soluble materials in limestone samples can be dissolved, generating pores. With the increase in dry-wet cycles, the number of pores in the rock cannot be increased significantly due to the decrease in the soluble materials in the limestone samples.

In a more acidic environment, the NMR signal intensity of the limestone samples is relatively strong, while the intensity becomes weaker as the pH gradually increases.

3.1.2. T_2 Spectrum Area Analysis. By observing the T_2 spectrum in Figure 4, it can be found that the peak positions of the T_2 spectrum before and after the dry-wet cycle are not entirely aligned. After the first dry-wet cycle, a large number of pores cannot be found in the relatively dense limestone samples, and there is relatively little liquid in the pores. However, after repeated dry-wet cycles, the areas of the second and third peaks expand, indicating that secondary pores are produced in the samples after soaking during the acid portion of the cycle, and these pores are filled with liquid. Comparing the T_2 spectrum area of the limestone samples longitudinally, the spectrum area after the first soak is approximately one-tenth the area after the fifth soak in the pH 3 solution. This can fully explain why strong acids are effective in degrading limestone. However, the T_2 spectrum area after the 10th dry-wet cycle does not increase significantly compared with that after the 5th cycle. This may be because with the increase in dry-wet cycles, the calcium sulfate produced by the reaction of the sulfuric acid-nitric acid mixture with the limestone blocks the further inward corrosion of the acid. Horizontally, it can be seen from Table 3 that the T_2 spectrum area at pH 3 is larger than those at pH 5 and 7 after 10 cycles of drying and wetting, indicating that the pores inside the limestone samples become more developed under the active environment of at pH 3. As the acidity increases, the degradation effect of limestone samples becomes more significant. It is possible that with the increase in the number of dry-wet cycles, the calcium sulfate produced from the reaction of the sulfuric acid- nitric acid mixture with the limestone blocks the acid from further inward corrosion. From a horizontal perspective, it can be seen from Table 3 that the T_2 spectrum area at pH 3 is greater than those of pH 5 and 7 under the same 10 dry-wet cycles, which indicates that inside the limestone samples, the pores become more developed at pH 3. This shows that the stronger the acidity is, the more obvious the degradation effect on limestone samples.

3.1.3. Porosity Characteristic Analysis. Rock porosity is a measure of the pores of the rock medium. It is the ratio of the pore volume of the medium to the total volume, usually expressed as a percentage. The difference in quality of the sample before and after immersion is obtained by measurement, and then the volume of the solution is approximated according to distilled water density. This depicts the

Table 4: T_2 spectrum area and porosity deterioration after different dry-wet cycles in different environments.

Action environment	pH=3		pH=5		pH=7	
Rock identifier	Q-10-2	Q-10-3	Z-10-1	Z-10-3	D-10-1	D-10-3
T_2 spectral area after soaking once	195.285	275.908	202.799	275.728	115.524	275.908
Test porosity/%	0.372	0.484	0.431	0.296	0.242	0.344
Average porosity/%	0.428		0.363		0.293	
T_2 spectral area after soaking 5 times	1882.802	1679.041	1932.526	1624.719	1556.554	2648.225
Converted porosity/%	0.830	0.69	0.664	0.389	0.363	0.477
Average porosity/%	0.76		0.526		0.42	
Porosity deteriorationμ/%	123.118	42.562	54.060	31.419	50.000	38.663
Average porosity deterioration$\bar{\mu}$/%	82.840		42.740		44.331	
T_2 spectral area after soaking 10 times	2055.573	2180.602	2393.511	1963.584	1492.498	2277.309
Converted porosity/%	1.100	0.901	0.682	0.537	0.380	0.654
Average porosity/%	1.005		0.609		0.517	
Porosity deteriorationμ/%	195.699	86.157	58.237	81.419	57.025	90.116
Average porosity deterioration$\bar{\mu}$/%	140.928		69.828		73.571	

Note: The calculation formula for porosity deterioration is $\mu = (\varphi_i - \varphi_0/\varphi_0) \times 100\%$; φ_0 is the initial porosity of the material, φ_i is the porosity of material damage after the i th dry-wet cycle.

Table 5: The changing conditions of the limestone mass loss rate after different numbers of dry-wet cycles in different environments.

Active environment	Rock sample no	Number of dry-wet cycles n					
		1		5		10	
		κ_m/%	Average	κ_m/%	Average	κ_m/%	Average
pH = 3	Q-10-1	0.24	0.18	0.64	0.68	1.15	1.09
	Q-10-2	0.14		0.79		1.07	
	Q-10-3	0.16		0.61		1.05	
pH = 5	Z-10-1	0.07	0.083	0.18	0.18	0.28	0.30
	Z-10-2	0.09		0.21		0.32	
	Z-10-3	0.09		0.15		0.31	
pH = 7	D-10-1	0.03	0.05	0.08	0.09	0.15	0.17
	D-10-2	0.06		0.09		0.18	
	D-10-3	0.06		0.11		0.17	

specimen's test porosity. The area of the curve in T_2 spectrum distribution is directly proportional to the volume of fluid in the pores of the rock. By establish the relationship between the known test porosity and the corresponding curve, we can deduce with the converted porosity of curves in other T_2 spectrum distribution. After the dry-wet cycle, the porosity corresponding to that known from NMR is converted to obtain information about the T_2 spectrum area and pore deterioration of the limestone samples after different numbers of dry-wet cycles in different environments (Table 4).

From Table 4, it can be observed that for the working environments of pH = 3, 5, and 7, after the first dry-wet cycle, the corresponding average porosities of the limestone samples are 0.428%, 0.363%, and 0.293%, respectively. The data show that after the first dry-wet cycle of limestone, the porosity of the limestone is negatively correlated with the pH of the corresponding soak solution. After 10 dry-wet cycles, the converted porosity increased significantly. In contrast, the porosity of the limestone samples has increased by 69.828% to 140.928% compared with the samples that experienced only one dry-wet cycle, indicating that fissures in the limestone increase greatly due to the dry-wet cycle. The average porosity of the limestone samples increased between 42.740% and 82.840% after 5 dry-wet cycles, and the average porosity of the limestone samples after 10 dry-wet cycles was higher than that after 5 dry-wet cycles. It has only increased by 20.379%–31.555%. The porosity of the limestone samples shows a decreasing trend with an increasing number of cycles. The average porosity of the limestone samples in Table 5 and the number of dry-wet cycles are taken to draw a bar chart, as shown in Figure 5, which shows that with the increase in dry-wet cycles, the growth rate of each bar in the chart gradually decreases. The porosity growth rate of the samples continues to decrease. Moreover, the stronger the acidic condition is, the faster the porosity growth of the samples.

Having experienced 10 dry-wet cycles in environments with pH values of 3, 5, and 7, the average porosity deterioration degrees of limestone samples are 140.928%, 69.828%, and 73.571%, respectively. Obviously, limestone is very sensitive to an acidic environment, which is closely related to the main mineral, calcite, in limestone. In an acidic environment, especially a strong acid environment, material exchange caused by the chemical reaction will directly destroy the initial structure of the minerals in the limestone samples. The connection between the crystal structure of the samples is destroyed, and the internal structure of the samples is greatly changed. At the same time, the pores in the limestone have increased significantly.

3.2. Analysis of the Physical Properties of the Corrosion Process

3.2.1. Mass Loss Rate. The chemical reaction of the dry-wet cycle process will result in exchanges of substances and changes in mass. The mass loss rate of the limestone samples is κ_m, which is used to evaluate the mass change of the limestone samples during the dry-wet cycle. Recall that the mass of the original samples after drying is m_0, the mass of the samples after each stage of dry-wet cycle drying is m_i, and the mass loss rate of the limestone samples is.

$$\kappa_m = \frac{m_0 - m_i}{m_0} \times 100\%. \quad (1)$$

Equation (1) is used to calculate the mass loss rates of the samples dried after soaking in different acidic environments, and the average value is taken after calculation to draw a histogram. It can be seen from Figure 6 that there are varying degrees of loss in the mass of the limestone after repeated dry-wet cycles under different pH values. Among these, the mass loss rate of limestone is largest at pH 3, and it is much larger than those of the other two pH soak solutions. In general, in each weighing interval, the increase in the mass loss rate of the limestone samples in the pH 3 solution is also the largest, and both the mass loss rate and increase have shown a downwards trend with the increase in pH.

3.2.2. Saturated Water Absorption. The saturated water absorption rate is used to evaluate the number of pores and the degree of opening and closing of the limestone under the action of the dry-wet cycle. Recall that the quality

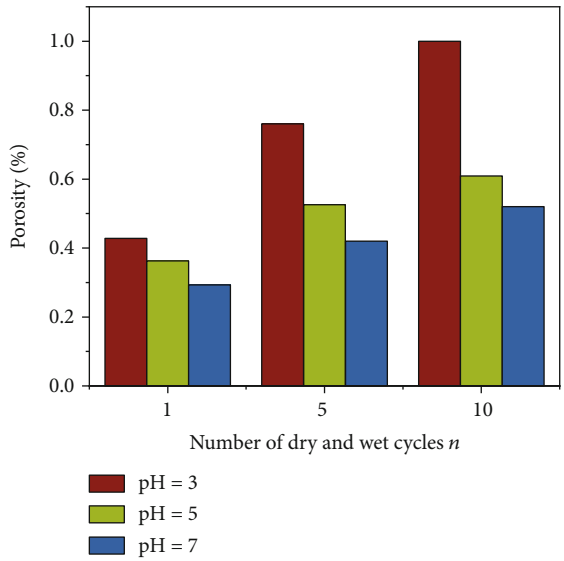

Figure 5: Relationship between average porosity and number of dry-wet cycles.

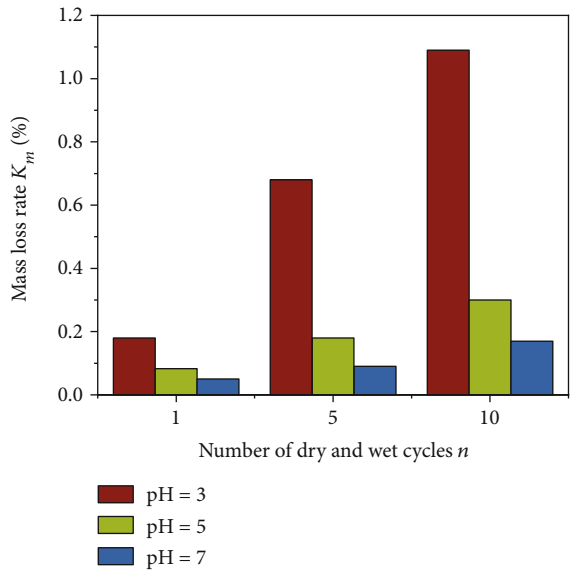

Figure 6: The relationship between mass loss rate and the number of dry-wet cycles.

of the limestone samples after vacuum saturation is m_{sa}, and the masses of the dried samples after the dry-wet cycle are represented by m_{dr}. The saturated water absorption rate of the limestone samples can be then expressed as

$$\omega_{sa} = \frac{m_{sa} - m_{dr}}{m_{dr}} \times 100\%. \quad (2)$$

A bar chart between the saturated water absorption rate and the number of dry-wet cycles was drawn (Figure 7).

It can be found from the relationship diagram of the change in saturated water absorption that the water absorption of limestone in acid is not strong. After 10 dry-wet cycles, the average water absorption of the samples in an

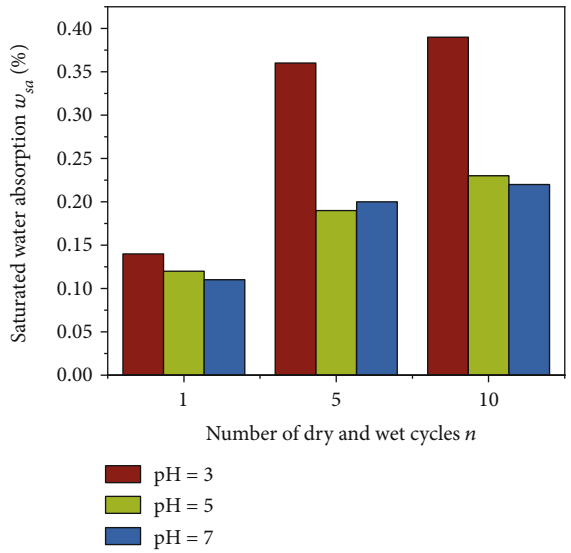

Figure 7: The relationship between saturated water absorption rate and the number of dry-wet cycles.

immersion environment of pH 3 is only 0.39%. From the first dry-wet cycle, the saturated water absorption rate of each stage of the dry-wet cycle is higher than that of the previous stage. From the overall trend of change, the increase is large in the early stage and gradually slows down in the later stage are shown in Table 6.

3.3. Chemical Analysis of the Corrosion Process. The analysis of the chemical properties of the corrosion process of the samples is measured by an inductively coupled plasma atomic emission spectrometer in the study. Limestone is a carbonate rock, and its main mineral component is calcite. When the acidic solution interacts with the samples, continuous ion exchange will occur. Therefore, the equipment can be used to determine the mass of metal elements in the reaction solution.

3.3.1. Element Mass Concentration Changes. In the soaking process of the sample dry-wet cycle test, the intensity of the chemical reaction decreases as the pH of the solution rises. Due to the dry-wet cycle process in this test, the pH of the solution was measured every 8 h and maintained at the initial value. For this reason, it is not appropriate to reflect the degree of rock deterioration through the measured pH change. To determine the deterioration degree of the limestone samples after continuous dry-wet cycles, the concentrations of the other elements generated were measured. Prior to the test, each limestone sample is soaked in a different beaker. These beakers are grouped by pH and the number of dry-wet cycles. The beaker identifier is aligned with the number of soaked limestone samples in it. Upon completing the 1st, 5th, and 10th dry-wet cycle tests, the original solution was immediately diluted and sent to the testing laboratory. The measurement results of the mass concentration of each main element are shown in Table 7.

Comparing the mass concentration of each element in Table 7, it can be found that in each test result, the mass

Table 6: The changing conditions of the limestone saturated water absorption rate after different numbers of dry-wet cycles in different environments.

Action environment	Rock sample no	Number of dry-wet cycles n = 1		5		10	
		ω/%	Average	ω/%	Average	ω/%	Average
pH = 3	Q-10-1	0.09	0.14	0.28	0.36	0.39	0.39
	Q-10-2	0.14		0.32		0.43	
	Q-10-3	0.19		0.48		0.36	
pH = 5	Z-10-1	0.16	0.12	0.25	0.19	0.26	0.23
	Z-10-2	0.10		0.18		0.23	
	Z-10-3	0.11		0.15		0.20	
pH = 7	D-10-1	0.09	0.11	0.14	0.20	0.15	0.22
	D-10-2	0.11		0.21		0.26	
	D-10-3	0.13		0.25		0.24	

Table 7: Results of the mass concentration of each main element after different dry-wet cycles.

Active environment	Beaker identifier	Mg/(mg/L)	Mg concentration increase/%	Ca/(mg/L)	Ca concentration increase/%	Fe/(mg/L)	Fe concentration increase/%
pH = 3	Q-1	0	—	311.3	—	19.6	—
	Q-5	8.7	—	784.6	152.04	27.1 30.	38.27
	Q-10	23.7	172.41	1155	47.21	30.6	12.92
pH = 5	Z-1	0	—	150.3	—	14.2	—
	Z-5	6.5	—	331	120.23	15.7	10.56
	Z-10	14.3	120	695	109.97	17	8.28
pH = 7	D-1	0	—	39.7	—	7.6	—
	D-5	0.6	—	166.5	319.40	13.8	81.58
	D-10	9.5	1483.33	332.8	99.88	12.5	-9.42

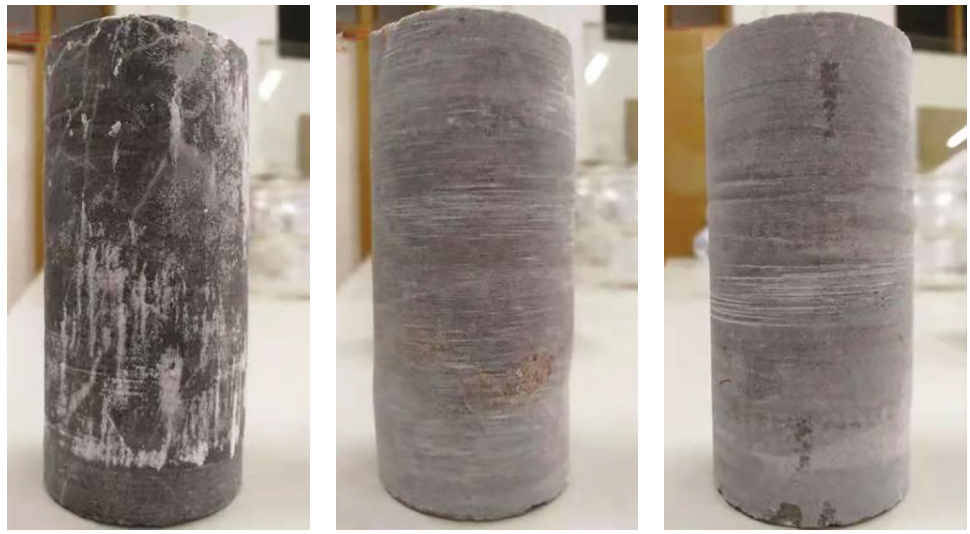

(a) pH = 3 (b) pH = 5 (c) pH = 7

Figure 8: Limestone samples after 10 dry-wet cycles in different acid solutions.

concentration of Ca is the highest, and it far exceeds the concentration of the other two elements. From the perspective of the increase in the element mass concentration after each dry-wet cycle, the increases in the element mass concentrations of Mg and Ca are relatively close. In addition, the element mass concentration increase of Mg is large after 10 dry-wet cycles, this may have been caused by the individual differences in the samples. In general, the mass concentrations of Mg, Ca, and Fe in the three groups of experiments increase with the increase in the number of dry-wet cycles. In addition, the lower the pH is, the greater the increase in the mass concentrations of each element. The concentration of each element in the reaction solution is positively correlated with the number of dry-wet cycles n and negatively correlated with the established pH.

The results of mineral composition analysis show that the limestone samples selected in this experiment are all limestone of relatively high purity. During the soaking process, calcite ($CaCO_3$), dolomite ($CaMg(CO_3)_2$, and CaFe $(CO_3)_2$) are the main materials involved in the reaction with the hydrogen ion H^+ in the solution. The ionic equation for the reaction of limestone with a sulfuric acid-nitric acid mixture is

$$CaCO_3 + 2H^+ \longrightarrow Ca^{2+} + H_2O + CO_2\uparrow \quad (3)$$

$$CaMg(CO_3)_2 + 4H^+ \longrightarrow Ca^{2+} + Mg^{2+} + 2H_2O + CO_2\uparrow \quad (4)$$

$$CaFe(CO_3)_2 + 4H^+ \longrightarrow Ca^{2+} + Fe^{2+} + 2H_2O + CO_2\uparrow \quad (5)$$

Figure 8 shows the limestone samples with 10 dry and wet cycles in acidic solutions of different pH values.

It can be seen from Figure 8 that after 10 dry-wet cycles, the morphologies of the samples after soaking in three different solutions are significantly different. When in distilled water with a pH of 7, the processing marks on the surface of the limestone are clear. In addition, the surface is mixed with slight yellowish brown mud, and the water-rock interaction is relatively weak. When the action environment changes to pH 5, the processing marks on the limestone surface are somewhat fuzzy, and the number on the surface of the samples is also somewhat fuzzy. A small amount of white particles is also attached to the whole body of the limestone. However, for the samples immersed in a strong acid environment with pH 3, most of its surface has been covered by white precipitates, and the number is difficult to distinguish.

4. Conclusions

This paper investigated the problem of rock deterioration and damage caused by the combination of acid rain and the changes between sunny and rainy weather. Rock samples experiencing different dry-wet cycles were taken for NMR measurements and inductively coupled plasma atomic emission spectrometer measurements. The conclusions are as follows.

(1) Having experienced corrosion in the acid solution, the pore sizes of the limestone gradually increase, and the whole T_2 spectral curve moves to the right. As the pH value decreases, the T_2 spectral curve presents a more pronounced right-moving tendency. In addition, the dry-wet cycle can result in the expansion of old fissures and the formation of new pores, and the generation rate of the new pores continues to decrease. With the increase in dry-wet cycles, the right-moving scope of the T_2 spectral curve gradually decreases

(2) The porosity of limestone is negatively correlated with the pH value of the corresponding soaking solution. With the increase in the dry-wet cycles, the growth rate of the limestone sample porosity decreases. Specifically, after 10 dry-wet cycles, the porosity increases by 69.828% to 140.928% compared with the first cycle and only increases by 42.740% to 82.840% compared with the fifth cycle

(3) The mass loss rate shows a decreasing trend with increasing pH, but the growth rate of the mass loss rate decreases as the number of dry-wet cycles increases. In addition, the saturated water absorption rate is positively correlated with the number of dry-wet cycles and has a negative relationship with pH

(4) After the dry-wet cycles, the mass concentration of each element in order from high to low in the original reaction solution is Ca, Mg, and Fe. The mass concentrations of these three elements increase with increasing dry-wet cycles. Moreover, the lower the pH is set during the reaction, the more rapid the mass concentration growth rate of each element

In summary, porosity, deterioration of pores, saturated water absorption rate, and mass loss rate are four indices used in this paper to define limestone deterioration and damage degree. The effect decreases with increasing of the pH of the soak solution. The deterioration of and degree of damage to limestone increases with increasing dry-wet cycles, while the growth rate of the degree decreases with increasing cycles. Through the research in this study, the results can provide some reference for local disaster prevention and mitigation work.

Data Availability

The data that support the findings of this study are available from the corresponding author upon reasonable request.

Conflicts of Interest

The authors declare that they have no known competing financial interests or personal relationships that could have appeared to influence the work reported in this paper.

Acknowledgments

The authors would like to acknowledge the financial support from the National Natural Science Foundation of China under Grant No. 52068016. The work in this paper was also supported by the Systematic Project of Guangxi Key Laboratory of Disaster Prevention and Structural Safety under Grant No. 2019ZDK023, the Guangxi Key Laboratory of Geomechanics and Geotechnical Engineering (Grant No.19-Y-21-9, 20-Y-XT-01), the High Level Innovation Team and Outstanding Scholar Program of Universities in Guangxi Province. (Grant No. 202006), and the Guangxi Natural Science Foundation under Grant Nos. 2020GXNSFAA297118 and 2020GXNSFAA159125.

References

[1] G. He, X. Zhao, and M. Yu, "Exploring the multiple disturbances of karst landscape in Guilin World Heritage Site, China," *Catena*, vol. 203, article 105349, 2021.

[2] S.-L. Li, C.-Q. Liu, J.-A. Chen, and S.-J. Wang, "Karst ecosystem and environment: characteristics, evolution processes, and sustainable development," *Agriculture, Ecosystems & Environment*, vol. 306, article 107173, 2021.

[3] A. Basu, B. K. Ram, N. K. Nanda, and S. S. Nayak, "Deterioration of shear strength parameters of limestone joints under simulated acid rain condition," *International Journal of Rock Mechanics and Mining Sciences*, vol. 135, article 104508, 2020.

[4] Z. Gan, X. Pan, H. Tang, J. Huang, S. Dong, and W. Hua, "Experimental investigation on mixed mode I-III fracture characteristics of sandstone corroded by periodic acid solution," *Theoretical and Applied Fracture Mechanics*, vol. 114, article 103034, 2021.

[5] X. Li, D. Qu, Y. Luo, R. Ma, K. Xu, and G. Wang, "Damage evolution model of sandstone under coupled chemical solution and freeze-thaw process," *Cold Regions Science and Technology*, vol. 162, pp. 88–95, 2019.

[6] T. S. Rötting, L. Luquot, J. Carrera, and D. J. Casalinuovo, "Changes in porosity, permeability, water retention curve and reactive surface area during carbonate rock dissolution," *Chemical Geology*, vol. 403, pp. 86–98, 2015.

[7] S. Jie, Z. Li, C. Huang, Z. Cao, Y. Xu, and Z. Chen, "Catastrophe mechanism of stress-fissure coupling field in mining close distance seams in Southwest China," *Geofluids*, vol. 2021, Article ID e8073602, 9 pages, 2021.

[8] J. Wang and Q. Yu, "Experimental investigations of the process of carbonate fracture dissolution enlargement under reservoir temperature and pressure conditions," *Geofluids*, vol. 2018, 19 pages, 2018.

[9] S. Xiao, C. Zeng, J. Lan et al., "Hydrochemical characteristics and controlling factors of typical dolomite Karst Basin in humid subtropical zone," *Geofluids*, vol. 2021, 14 pages, 2021.

[10] X. Yang, A. Jiang, and M. Li, "Experimental investigation of the time-dependent behavior of quartz sandstone and quartzite under the combined effects of chemical erosion and freeze-thaw cycles," *Cold Regions Science and Technology*, vol. 161, pp. 51–62, 2019.

[11] N. Alsaaran and G. A. Olyphant, "A model for simulating rock-water interactions in a weathering profile subjected to frequent alternations of wetting and drying," *Catena*, vol. 32, no. 3-4, pp. 225–243, 1998.

[12] K. Beck and M. Al-Mukhtar, "Cyclic wetting–drying ageing test and patina formation on tuffeau limestone," *Environmental Earth Sciences*, vol. 71, no. 5, pp. 2361–2372, 2014.

[13] B. Du, Q. Cheng, L. Miao, J. Wang, and H. Bai, "Experimental study on influence of wetting-drying cycle on dynamic fracture and energy dissipation of red-sandstone," *Journal of Building Engineering*, vol. 44, article 102619, 2021.

[14] W. Hua, S. Dong, Y. Li, and Q. Wang, "Effect of cyclic wetting and drying on the pure mode II fracture toughness of sandstone," *Engineering Fracture Mechanics*, vol. 153, pp. 143–150, 2016.

[15] W. Hua, S. Dong, Y. Li, J. Xu, and Q. Wang, "The influence of cyclic wetting and drying on the fracture toughness of sandstone," *International Journal of Rock Mechanics and Mining Sciences*, vol. 78, pp. 331–335, 2015.

[16] Q. Jiang, H. Deng, J. Li et al., "The degradation effect and mechanism by water-rock interaction in the layered sandstone in the Three Gorges reservoir area," *Arabian Journal of Geosciences*, vol. 12, no. 23, p. 722, 2019.

[17] S. Jiang, M. Huang, X. Wu, Z. Chen, and K. Zhang, "Deterioration behavior of gypsum breccia in surrounding rock under the combined action of cyclic wetting-drying and flow rates," *Bulletin of Engineering Geology and the Environment*, vol. 80, no. 6, pp. 4985–5001, 2021.

[18] N. Zhao and H. Jiang, "Mathematical methods to unloading creep constitutive model of rock mass under high stress and hydraulic pressure," *Alexandria Engineering Journal*, vol. 60, no. 1, pp. 25–38, 2021.

[19] D. Yang, H. Jianhua, and X. Ding, "Analysis of energy dissipation characteristics in granite under high confining pressure cyclic load," *Alexandria Engineering Journal*, vol. 59, no. 5, pp. 3587–3597, 2020.

[20] G. Su, G. Zhao, J. Jiang, and X. Hu, "Experimental study on the characteristics of microseismic signals generated during granite rockburst events," *Bulletin of Engineering Geology and the Environment*, vol. 80, no. 8, pp. 6023–6045, 2021.

[21] L. Obert, S. L. Windes, and W. I. Duvall, *Standardized Tests for Determining the Physical Properties of Mine Rock. RI-3891*, Bureau of Mines, U.S. Dept. of the Interior, 1946.

[22] A. B. Hawkins and B. J. McConnell, "Sensitivity of sandstone strength and deformability to changes in moisture content," *The Quarterly Journal of Engineering Geology*, vol. 30, p. A80, 1993.

[23] P. Ying, Z. M. Zhu, L. Ren et al., "Deterioration of dynamic fracture characteristics, tensile strength and elastic modulus of tight sandstone under dry-wet cycles," *Theoretical and Applied Fracture Mechanics*, vol. 109, article 102698, 2020.

[24] Z. L. Zhou, X. Cai, D. Ma, L. Chen, S. F. Wang, and L. H. Tan, "Dynamic tensile properties of sandstone subjected to wetting and drying cycles," *Construction and Building Materials*, vol. 182, pp. 215–232, 2018.

[25] S. B. Huang, Y. B. He, X. W. Liu, and Z. K. Xin, "Experimental investigation of the influence of dry-wet, freeze-thaw and water immersion treatments on the mechanical strength of the clay-bearing green sandstone," *International Journal of Rock Mechanics and Mining Sciences*, vol. 138, article 104613, 2021.

[26] Z. X. Zeng, L. W. Kong, M. W. Wang, and J. T. Wang, "Effects of remoulding and wetting-drying-freezing-thawing cycles on the pore structures of Yanji mudstones," *Cold Regions Science and Technology*, vol. 174, article 103037, 2020.

[27] D. Zhang, A. Q. Chen, X. M. Wang, and G. C. Liu, "Quantitative determination of the effect of temperature on mudstone decay during wet-dry cycles: a case study of 'purple mudstone' from south-western China," *Geomorphology*, vol. 246, pp. 1–6, 2015.

[28] L. Q. Wang, Y. P. Yin, B. L. Huang, and Z. W. Dai, "Damage evolution and stability analysis of the Jianchuandong dangerous rock mass in the Three Gorges Reservoir Area," *Engineering Geology*, vol. 265, article 105439, 2020.

[29] Z. Q. Luo, W. Wang, Y. G. Qin, and J. Xiang, "Early warning of rock mass instability based on multi-field coupling analysis and microseismic monitoring," *Transactions of the Nonferrous Metals Society of China*, vol. 29, no. 6, pp. 1285–1293, 2019.

[30] A. Potysz, W. Bartz, K. Zboińska, F. Schmidt, and M. Lenz, "Deterioration of sandstones: Insights from experimental weathering in acidic, neutral and biotic solutions with Acidithiobacillus thiooxidans," *Construction and Building Materials*, vol. 246, article 118474, 2020.

[31] D. Camuffo, "Acid rain and deterioration of monuments: how old is the phenomenon?," *Atmospheric Environment. Part B. Urban Atmosphere.*, vol. 26, no. 2, pp. 241–247, 1992.

[32] L. L. Cui, J. H. Liang, H. B. Fu, and L. W. Zhang, "The contributions of socioeconomic and natural factors to the acid deposition over China," *Chemosphere*, vol. 253, article 126491, 2020.

[33] Z. Zheng and C. Y. Hong, "Electron microscope analyses of insoluble components in acid rain, Guilin City, China," *Atmospheric Research*, vol. 32, no. 1-4, pp. 289–296, 1994.

[34] R. Ulusay, "The isrm suggested methods for rock characterization, testing and monitoring: 2007-2014," *Springer International Publishing*, vol. 15, no. 1, pp. 47-48, 2014.